

Aerodynamic Drag Computation of Lower Earth Orbit (LEO) Satellites

Abdul Majid¹, Muhammad Naeem Owais¹, Muhammad Nauman Qureshi²

Abstract—In general estimated constant drag coefficient is used for the dynamic modeling of satellites in an orbit. This causes uncertainties in the prediction of satellite orbital perturbations. In the past few decades, seldom requirement is being observed in the precise determination of the drag coefficient of spacecraft. It was justified because of lack in the experimental validation of the theory. However, with the advancement on new atmospheric models of enhanced accuracy have abled a better classification of the drag force. The standard fluid dynamics computational techniques based on Navier-Stokes equations and empirical codes for aerodynamic computations are valid only in the continuum region. For altitudes more than ~ 120 km, the atmosphere is rarefied and the transport terms in the Navier-Stokes equations of continuum gas dynamics fail due to insufficient collision between the molecules. This happens when gradients of the macroscopic variables become so steep that their scale length is of the same order as the average distance travelled by the molecules between collisions, or mean free path. To accurately predict the aerodynamic characteristic of satellites flying at such higher altitudes, the available numerical techniques are discussed and presented in detail. The results computed based on these models are compared with the DS2V code by GA Bird. In order to see the effect of drag coefficient with different velocities and altitudes, simulations have also been done for a satellite in low earth orbit initially at 300 km altitude.

I. INTRODUCTION

Spacecraft trajectories are predicted and determined by using the knowledge of upper atmosphere. The orbital energy of a spacecraft is reduced by the action of drag force which results from the exchange of momentum between the spacecraft and the upper atmosphere^[1].

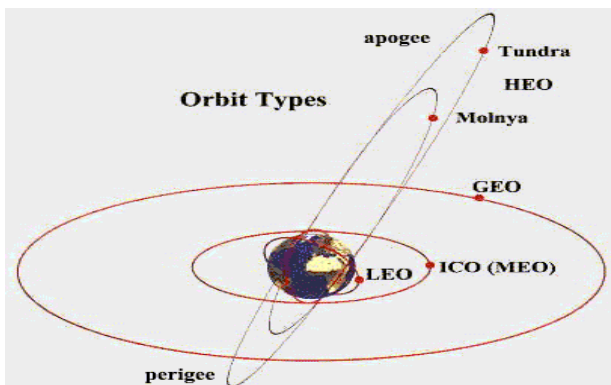


Figure 1: Types of earth orbits

The earth orbits is usually categorized according to the altitude from earth surface such as Lower Earth Orbit (LEO), Medium Earth Orbit (MEO), Geosynchronous Earth Orbit (GEO), Highly Elliptical Orbit (HEO) and Lagrange Point Orbit. Each orbit has specific purpose to serve. However, in this current paper the discussion is kept till LEO only. The orbit types is shown in the Fig. 1.

LEO orbits are closest to the earth with an orbital altitude in the range of 180 – 2000 km, the time period is between 90 – 110 minutes (13 and 15 times/ day) and it has high orbital velocities. LEO is most populous of them having large number of operating satellites as shown in Fig. 2.

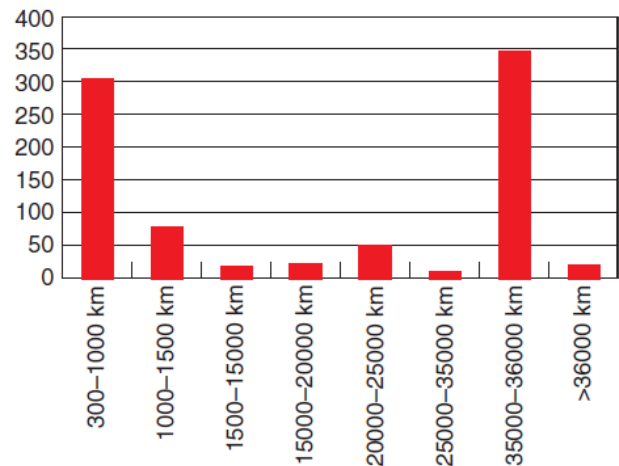


Figure 2: Number of satellites operating at various altitudes ^[4]

The reason for the increased number of satellites in LEO is its multipurpose applications. These applications include earth observation, weather monitoring, remote sensing, technology and astronomy. International Space Station (ISS) and Hubble Space Telescope also operate in this region. Apart from advantages, there are also some drawbacks of the satellites orbiting in LEO for instance it is the most populated region with more than 10,000 objects with a size of over 10 cm. It also provides low coverage area (< 4000 km) and, most importantly, it is more prone to the effects caused by the atmospheric drag. The resident space object detections using Navspasur Radar is depicted in Fig. 3.

Abdul Majid and Muhammad Naeem Owais are with the Space and Upper Atmospheric Research Commission, Karachi, Pakistan.
Muhammad Nauman Qureshi is with the DHA Suffa University, Karachi, Pakistan.

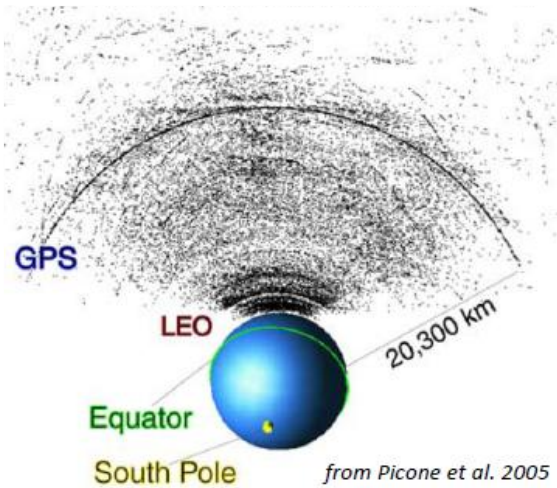


Figure 3: Resident space object detections using Navspasur Radar (from Picone et al. 2005) [2]

The satellite has to overcome the environmental disturbances torques that hamper its smooth functionality. These torques are Gravity Gradient Torque, Solar Radiation Torque, Geo-Magnetic Field Torque and Aerodynamic Torque. These disturbances depends mainly on their distances from earth as mentioned below in the Table 1.

Table 1: Environment Disturbance Torques [3]

Sr. No	Source	Dependence on earth distance	Region of space where dominant
1.	Aerodynamic	$e^{-\alpha r}$	Absolute below ~500 km
2.	Magnetic	$1/r^3$	~500 km to ~35,500 km
3.	Gravity Gradient	$1/r^3$	Out to about synchronous altitude
4.	Solar Radiation	Independent	Interplanetary space above synchronous altitude

Atmospheric drag has an influence on all satellites and is one of the key parameter responsible for the orbital perturbation.

This drag does has an influence at all altitudes ranging from low earth orbit to beyond geostationary altitudes. Aerodynamic analysis of satellites is necessary to predict the drag force perturbation to their orbital trajectory, which for LEO orbits is the second in magnitude after the gravitational disturbance due to the Earth's oblateness.

The drag models also assist for accurate orbit determination, mass or weighing estimation and analysis of geophysical phenomenon. The accurate orbit determination and mass of satellite are time critical and results are available within few hours. These results may assist for improvement in the drag models.

It is evident from table 1 that the effects of aerodynamic disturbances is more prominent at altitude below 500 km. This is also the region where ISS lies so the need of precise computation of the aerodynamic drag on the satellite in this region is essential. The satellite suffers from unwanted perturbing torques which need to be controlled by an appropriate attitude and orbit control system AOCs such as reaction wheels or momentum

wheels. However, these devices are very costly and requires precise modelling of the disturbances.

Also in LEOs, when considering the motion over long duration the earth's atmosphere cannot be neglected because the air density (the order of magnitude is $\rho = 10^{-11}$ kg/m³ at 400 km altitude) is depending solely on altitude but also varies according to the solar activity and the geomagnetic index [4].

The atmosphere around 120 km above earth is considered as rarefied. The standard Computational Fluid Dynamics (CFD) and aerodynamic analysis techniques are valid only in continuum atmosphere or for the altitude below 90 km. Therefore these techniques cannot be used for calculating drag forces acting on satellites orbiting in LEO or above orbits. Therefore it is essential to move to the some other models based on microscopic properties of gas. The microscopic models also called molecular models that consider gas as myriad of discrete molecules.

In recent times, the trend of research for the determination of spacecraft drag modelling is on increase despite all the difficulties. The accurate modelling of the drag has a direct impact on the success of the mission and orbital determination. A better model will enable to observe new mission concepts in which this atmospheric drag plays a vital role [1].

The current study is focused on the numerical techniques based on the microscopic approach are used for calculating drag forces acting on the satellites.

II. THEORETICAL BACKGROUND

This paper focuses on the thermospheric atmospheric region which is a high altitude layer that exist above 85 km. This layer can be further divided into two parts. The temperature increase at its lower part (below around 200 km) because of the absorption of EUV energy from the sun. While in the upper part, the increase in temperature ultimately reaches a limiting value (exospheric temperature) and does not change with height because of the effect known as the infrequency of intermolecular collisions that occurs at very low density. The temperature and neutral density vary with the amount of energy received by the thermosphere. Generally, the solar flux and the geomagnetic activity are the main energy sources affecting its structure [1].

III. FREE MOLECULAR FLOW

The extremely low level of oxygen in the atmosphere of LEO demands a different aerodynamics methodology than that used in the continuum regime. The flow regime of LEO spaceflight is commonly described as free molecular because of its very low density. It means that the mean-free path, indicated in Fig. 4, is considerably larger in comparison with the characteristic dimension of the object contained in that flow. As a result, there is extremely low possibility of molecules collisions in the flow field around the body and the flow can be judiciously assumed collisionless and it cannot be further considered as a continuum medium anymore.

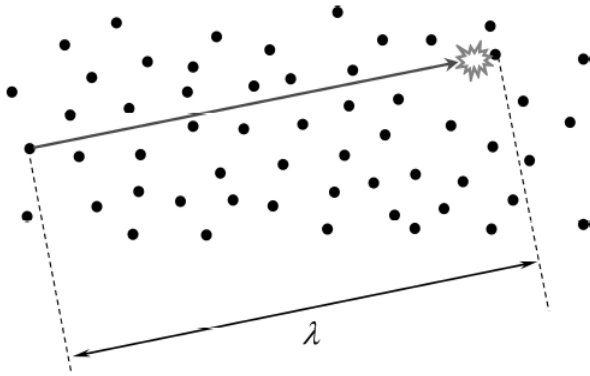


Figure 4: Molecular mean free path [1]

To quantify the validity of the collisionless assumption or the degree of rarefaction of a gas is generally expressed through a non-dimensional parameter known as Knudsen number (Kn), which is the ratio of the mean free path λ to the characteristic dimension L , i.e.

$$k_n = \lambda / L \tag{1}$$

The traditional requirement for the Navier-Stokes equations to be valid is that Knudsen number should be less than 0.1. The errors in the Navier-Stokes result is significant in the regions of the flow where the approximately defined local number exceeds 0.1, and the upper limit on the local Knudsen number at which the continuum model must be replaced by the molecular model may be taken to be 0.2.

The transport terms vanish in the limit of zero Knudsen number and the Navier-Stokes equations then reduce to the inviscid Euler equations. The flow is then isentropic from the continuum viewpoint, while the equivalent molecular viewpoint is that the velocity distribution function is everywhere of the local equilibrium of Maxwellian form. The opposite limit of infinite Knudsen number is the *collision less of free molecular* flow regime. These Knudsen limits on the conventional mathematical formulations are shown schematically in Fig. 5 [5].

II.II. FLOW REGIMES

Globally flow can be characterized or divided into following regimes on the basis of the Knudsen number:

If $Kn < 0.01$: The region is categorized as continuum region and Navier-Stokes equations hold good. One can take flow as continuum which is dominated as by intermolecular collisions.

If $0.01 < Kn < 10$: The region is characterized as Transitional regime and here both intermolecular and molecule-surface collisions are important. Here mean free path is neither too small for the Navier-Stokes equations to be valid nor too large to be declare as free molecular regime.

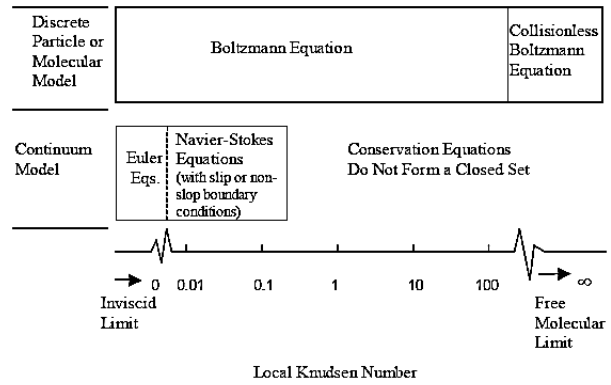


Figure 5: The Knudsen number limits on the mathematical models [1]

If $Kn > 10$: The region is considered as free molecular regime. Free molecular is dominated by molecule-surface interaction with negligible interaction between incident and reflected particles.

In brief, a high Kn indicates the importance of the particulate nature of the fluid and that the Boltzmann equations must be employed, whereas a low Kn permits treatment of fluid as a continuum and the use of the Navier-Stokes equations. For the moderate values of Kn, there is need to develop bridging relations among continuum & rarefied.

II.III. NUMERICAL METHODS

Certain numeric methods are used for the calculation of aerodynamic coefficients of the complex bodies. In a free molecular flow, the four main computational methods used for analyzing the aerodynamics of a body are as follows:

- i) Panel Method
- ii) Ray-Tracing Panel Method (RTP)
- iii) Test-Particle Monte Carlo (TPMC)
- iv) Direct Simulation Monte Carlo (DSMC)

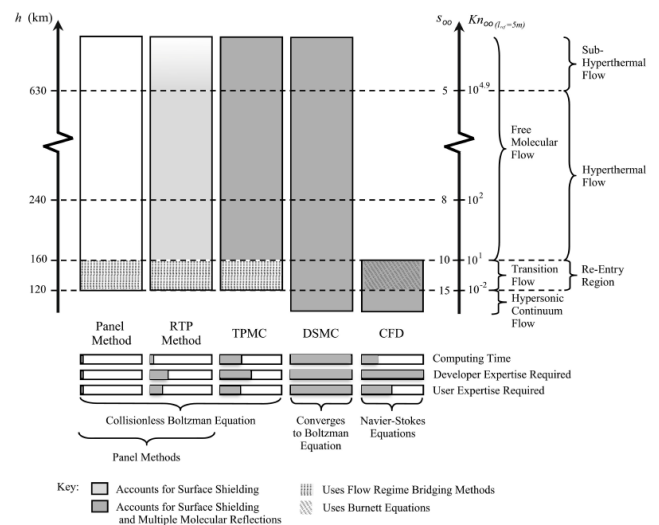


Figure 6: Comparison of existing computational approaches to spacecraft dynamics in LEO [1]

The comparison among them is shown in Fig. 6^[1,8], along with the Computational Fluid Dynamics (CFD). The free stream molecular speed ratio s and free stream Knudsen number Kn is represented by the right-hand axes in the figure. The Kn is based on a spacecraft with a characteristic dimension of 5 m. The Kn scale is used to depict the different regimes of rarefied flow^[1]. This paper focuses only DSMC method.

II.IV. MATHEMATICAL MODELING

There are different techniques available for solving the problem of calculating satellite drag in free molecular atmosphere. The most rigorous method is based on the Boltzmann equation^[9]. However keeping in view, the complexities and time involved in using rigorous methods comprising of complex differential equations, for the current study equations provided by the GA Bird^[5] are used for the numerical simulation of drag estimation of satellite in an orbit.

$$\frac{p}{p_\infty} = \left[(1+\varepsilon) \cdot \pi^{-1/2} \cdot s \cdot \sin(\theta) + 1/2 \cdot (1-\varepsilon) \cdot \sqrt{\left(\frac{T_r}{T_\infty}\right)} \right] \cdot \exp(-s^2 \sin^2(\theta)) \quad (2)$$

$$+ \left[(1+\varepsilon)(1/2 + s^2 \sin^2(\theta)) + 1/2 \cdot (1-\varepsilon) \cdot \sqrt{\left(\frac{T_\infty}{T_r}\right)} \cdot \pi^{1/2} \cdot s \cdot \sin(\theta) \right] \cdot [1 + \text{erf}(s \cdot \sin(\theta))]$$

Local values of pressure coefficient can be determined from the following relations (1). If we consider fraction ε of the molecules reflected specularly and the remaining fraction $1-\varepsilon$ is reflected diffusely. Then we will integrate these equations all over the body to calculate the aerodynamic coefficients.

The pressure coefficient related to this pressure ratio by

$$C_p = (P/P_\infty) - 1 \times 1/s^2 \quad (3)$$

The general result for the shear stress is

$$\frac{\tau}{p_\infty} = \pi^{-1/2} (1-\varepsilon) \cdot s \cdot \cos(\theta) \cdot \dots \dots \dots \left[\exp(-s^2 \sin^2(\theta)) + \pi^{1/2} \cdot s \cdot \sin(\theta) \cdot \{1 + \text{erf}(s \cdot \sin(\theta))\} \right] \quad (4)$$

The local skin friction coefficient is defined by

$$C_f = \tau / p_\infty / S^2 \quad (5)$$

The overall shear stress is zero for fully specular reflection and is entirely due to the incident molecules when the reflection is fully diffuse.

A. Drag coefficient computation

The algorithm developed for the implementation of (2) to (5) required geometric information of object for the determination of angle θ . Currently geometric information

in 3D form with triangular mesh is provided as input to the code.

The Force acting on an element results from the local pressure p acting over incremental area ds in the direction of the unit normal inward $-\mathbf{n}$.

$$\Delta C_F = -C_p \hat{\mathbf{n}} ds \quad (6)$$

The unit inward normal indicates the side of the element which is exposed to the flow. Vehicle component forces, which are in the body axis systems, are obtained by summing;

$$C_F = -\int_s C_p \hat{\mathbf{n}} ds \quad (7)$$

Force in each direction can be written as

$$C_A = S_{ref}^{-1} \sum C_p \hat{\mathbf{n}}_x A$$

$$C_Y = S_{ref}^{-1} \sum C_p \hat{\mathbf{n}}_y A \quad (8)$$

$$C_N = S_{ref}^{-1} \sum C_p \hat{\mathbf{n}}_z A$$

the drag coefficient is then calculated as

$$C_D = C_A \cos \alpha \cos \beta + C_Y \cos \alpha \sin \beta + C_N \sin \alpha \quad (9)$$

B. Maxwell Model

A detail description is available from GA Bird^[5] about the above relation. However, here we will explain only necessary terms involved for the computation of pressure and skin friction distribution all over the body.

Maxwell Model: For the flux distribution all over the body, the Maxwell model is the most widely used and is based on classical thermodynamics in which it is assumed that molecules will either reflect diffusely from a surface with complete energy accommodation or will reflect specularly with no change in energy^[10]. This model is presented in Fig. 7.

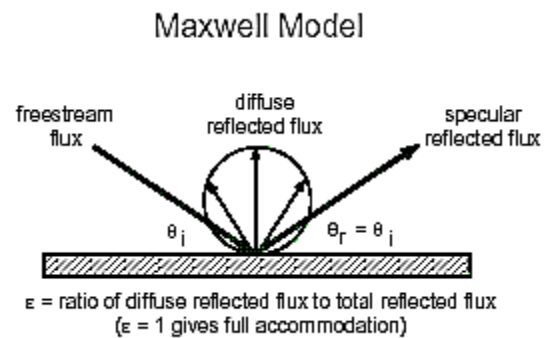


Figure 7: Description of Maxwell Model^[11]

i) Specular Reflection

In Fig. 8, we can see the specular deflection of incident molecules. The incident molecules are striking the surface at an angle of α and reflected back with the same angle and its tangential component is conserved.

ii) Diffuse Reflection

Here the reflected molecules are quite different from the incident and velocity and angle of reflected molecule has no concern with the incident one. It depends on the wall surface interaction and follows the Maxwellian distribution as shown in Fig. 9.

iii) Incident Angle

The angle of incidence α is the angle between the unit normal vector to the surface and the direction of free stream velocity.

iv) Speed Ratio

The speed ratio is defined as

$$s = V / (2RT)^{0.5} \quad (10)$$

It can also be written in more appropriate form and this form of relation is used for numerical calculations.

$$s = M(\gamma/2)^{0.5} \quad (11)$$

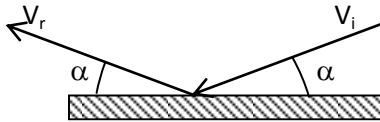


Figure 8: Description of specular reflection

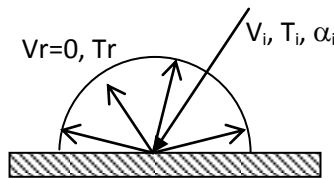


Figure 9: Description of diffuse reflection

v) Error Function

$\text{erf}(x)$ is the error function which is defined as

$$\text{erf}(a) = \frac{2}{\sqrt{\pi}} \int_0^a \exp(-x^2) \cdot dx \quad (12)$$

vi) Angle θ

As discussed before, this is the angle between inward normal and free stream wind vector. In modified Newtonian theory, we use this angle only for the exposed

area and for the shaded area; we declare this angle is equal to zero. But, here it has different sense, because above relation holds good all over the body and here we don't need to compute the shadow areas. So we will integrate this equation all over the body and we will local values all over the body (not only in the exposed area).

III. VERIFICATION & VALIDATION

A Numerical code is developed based on the above described equations. Verification and validation is the one of most important part of the work done, no matter it is in the form of numerical work or experimental work. Therefore the code developed is also validated with the known available techniques or methods.

A. Drag Coefficient of Flat Plate

The equation (13) may be applied directly to determine the drag coefficient on a thin flat plate at incidence α in stream of speed ratio s . The equations apply to the lower surface for positive values of α and to the upper surface for negative values of α . The upper surface pressure may be subtracted from the lower surface pressure to obtain the net force per unit area and we can have normal and parallel force coefficient. These normal and parallel force coefficients may now be resolved into the directions normal to and parallel to the stream direction in order to obtain the lift and drag coefficients for the flat plate. The reference area is based on the plan form area.

$$\begin{aligned} C_D = & 2 \frac{\{1 - \varepsilon \cos(2\theta)\}}{\pi^{1/2} s} \exp(-s^2 \sin^2(\theta)) \cdot \\ & + \frac{\sin(\theta)}{s} \left[1 + 2 \cdot s^2 + \varepsilon \{1 - 2 \cdot s^2 \cos(2\theta)\} \right] \cdot \text{erf}(s \cdot \sin(\theta)) \\ & + \frac{1 - \varepsilon}{s} \pi^{1/2} \sin^2(\theta) \sqrt{\frac{T_r}{T_w}} \end{aligned} \quad (13)$$

The results of drag coefficient computed from (9) and from the code are compared and presented in Fig. 10. The results from both methods are in a good accordance with each other. This verifies that the model implemented in the code.

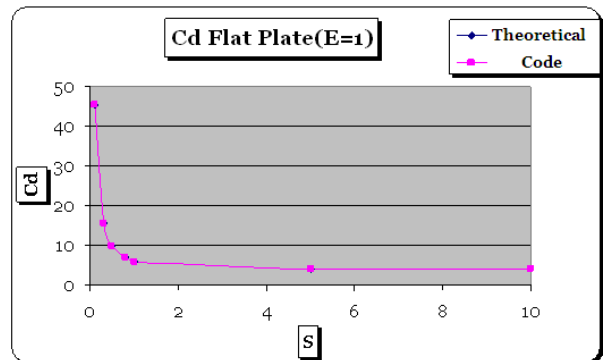


Figure 10: Drag coefficient comparison of flat plate

B. Drag Coefficient of Sphere

To validate the capability of code for three dimensional objects, we also compared the results with other 3D objects. Bird [5] provided the relation to determine the drag on a sphere in rarefied region, which is as followings:

$$C_D = \frac{2s^2 + 1}{\pi^{0.5}s^3} \exp(-s^2) + \frac{4s^4 + 4s^2 - 1}{2s^4} \operatorname{erf}(s) + \frac{2(1 - \varepsilon)\pi^{0.5}}{3s} \left(\frac{T_w}{T_\infty}\right)^{0.5} \quad (14)$$

The pressure distribution on a sphere is shown in Fig. 11. It is very clear from the plot that at stagnation point pressure coefficient is the maximum and keeps on decreasing as we move far from this point.

Drag for sphere is computed by using (14) and also for the code. The comparison plot is presented in Fig. 12. The results from both the codes are very close to each other.

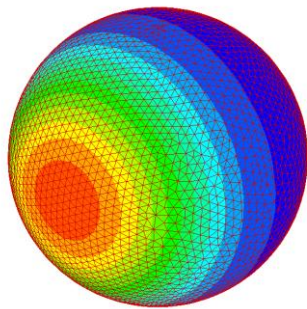


Figure 11: Pressure distribution on sphere

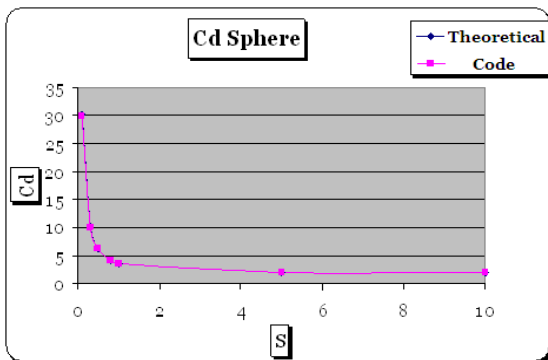


Figure 12: Drag coefficient comparison of sphere

IV. COMPARISON WITH DS2V CODE

The DS2V code of GA Bird is also used for comparison and verification of the code. This program is freely available [6] and known to be one of the wide spread codes. This code is based on DSMC (Direct Simulation Monte Carlo) approach that directly simulates molecules. Each simulated molecule represents 10^{12} to 10^{20} real molecules [1]. It is the only feasible numerical method

capable of computing flows in the range between the continuum and free molecular regimes, and is thus the method of choice for high-altitude flow field calculations [4,7]. However, the density of the gas is in direct proportion with its computational load [1].

In the regime of denser atmosphere, application of the Navier–Stokes and Euler equations is more efficient. Models based on the Navier–Stokes equation have been proved useful up to Knudsen numbers of $Kn = 0.3$ when extended by suitable models such as slip flow [4].

DSMC technique is based on the modeling of a real gas by millions of simulated molecules [11]. The velocity components and position coordinates of these molecules are stored in the computer and are modified with time as the molecules are concurrently followed through representative collisions and boundary interactions. This physical approach is fundamentally different from conventional CFD which seeks to obtain a numerical solution of a mathematical model of the gas- generally the Navier-Stokes equations [12]. The computational task associated with the direct physical simulation becomes feasible when the density of the gas is sufficiently low or the physical dimensions of the flow field are sufficiently small [13].

The simulations are made on a sphere at an altitude of 300km and the inflow velocity is taken as 7800 m/s. The results are shown in Fig 13. The drag coefficient computed by DS2V code is 2.059 and from the current code is 2.13. The different is only around 3% which shows that code developed gives fairly good results.

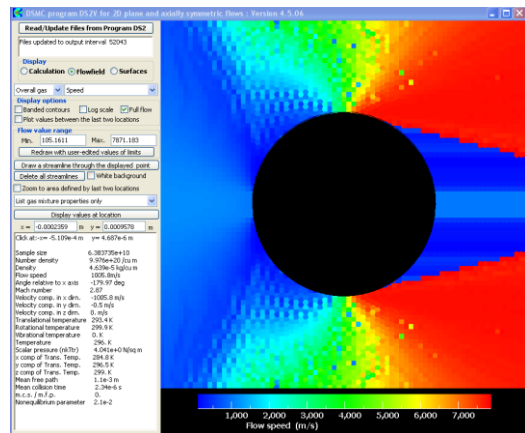


Figure 13: Flow field simulation using DS2V code

V. DRAG COEFFICIENT OF A SATELLITE

The theoretical background of the code and used for the calculation of satellite drag is explained in detail [2] and in section III. The verification and validation is also presented there. For the current calculation, a cube with a dimension of 1m on each side is taken as an exemplary satellite. In Fig. 14 the cube is shown with triangular surface meshing that is the requirement of the code for the geometric description of object. The simulation is made assuming altitude of 300 km and velocity of 7725 m/s (a typical value for a satellite orbiting in LEO). The pressure distribution is shown in Fig. 15. The drag coefficient computed based on these data is found to be 2.399812. It is very important here to mention that usually standard values of drag from literature are taken for satellite

ballistic coefficient computation, which may vary from the actual values. These variations may lead to wrong calculation of orbital life. Therefore it is recommended to use some numerical tool or sophisticated method to determine as good as possible values of drag. It is worthy to mention here that the value of drag is a function of velocity and altitude. The drag value varies with respect to change in these parameters. Usually one standard value of drag is taken that is also not recommended.

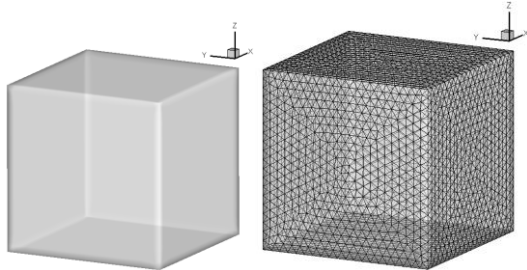


Figure 14: Cube with triangular surface meshing

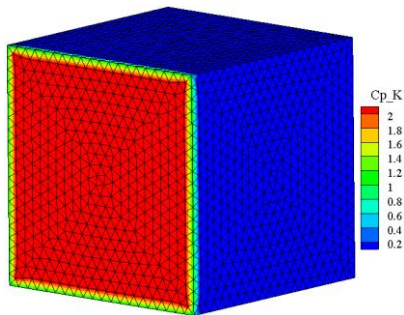


Figure 15: Pressure distribution on a cube in LEO

A. Drag estimation at different orbital altitudes and velocities

In order to see the variation in drag values at different altitude and velocities, a parametric analysis is presented here. It is important to make such parameters analysis so that variation in drag values during orbital decay could be estimated and evaluated. The variation in drag values at different altitudes and velocities in LEO orbit is shown in Table 1. The values of Mach number and Knudsen number corresponding to these conditions are around 12.3 and 2595 respectively. From this table it is clear that as the velocity varies or attitude changes, the value of drag coefficient also changed. At higher altitudes and higher velocities, the value of drag is lower as compared to lower altitudes and velocities. The main reason for this variation is the change in atmospheric density.

TABLE 2: VARIATION IN DRAG VALUES AT DIFFERENT ALTITUDES

		Height (km)			
		400	300	200	120
Velocity (m/s)	8000	2.38974	2.38575	2.36043	2.23219
	7700	2.40529	2.40114	2.37478	2.24137
	7400	2.42212	2.41780	2.39032	2.25130
	7100	2.44042	2.43590	2.40721	2.26208

VI. CONCLUSION

Even decades after the first artificial satellite put in orbit in 1957, the prediction of aerodynamic drag characteristics of an orbiting spacecraft still requires enormous efforts. There is still areas of improvement based on the emerging knowledge of the upper atmosphere environment as well as the understanding of the gas-surface interaction phenomena. In the last few years, an increasing trend in this research area is observed with the augmentation in the number of scientific missions with dedicated payloads and also the number of published literatures. A complex method to accurately predict the atmospheric drag for spacecraft is computed and compared in this paper.

The effects of aerodynamic drag on a satellite orbiting earth in LEO is being studied. The code shows good agreement with the available code and literatures. The behavior of drag value is closely observed by making a matrix between varying velocities and orbit altitudes. For a constant altitude, the values of drag indicate an inverse behavior with respect to the velocity and maximum drag value is observed at the minimum value of velocity.

Drag has a very high value at very low speed ratios. It shows a sharp decline in drag values till the speed ratio is 1. However, for value of speed ratio greater than 1 its shown gradual decrease in drag value.

It can also be concluded that at a constant velocity, the drag value shows a direct relation with satellite altitude having greater value at higher altitudes and vice versa.

Usually the standard and constant drag values are taken for orbital simulations of satellite. However the actual values of satellite can also be calculated and modelled in the trajectory software. Therefore, it is recommended to use values of actual drag coefficient values for orbital simulations.

The current study also revealed that the value of drag is not constant. It varies with altitude and velocity.

The velocity of satellites at LEO are more than 7000 m/s and a slight error in the estimation of values for simulating trajectory might lead to catastrophic results. The modeling with estimated value of drag might work fairly for polar orbits which remains at a constant altitude from earth throughout its life span. However, in the case of elliptical or highly elliptical orbit case the simulation with constant estimation of drag value will not come up with a reasonable results as in this case the value of drag is constantly varying.

The results obtained by the current study might be used to improve the code for trajectory simulation and mission analysis for satellites operating in LEO. The bench mark is set for the drag value analysis of simpler design or basic shape design of satellite models. However, the future work might be to carry out the same work but with more complex and realistic geometries of satellites.

VII. REFERENCES

- [1] Spacecraft Drag Modelling, David Mostaza Prieto; Benjamin P. Graziano; Peter C. E. Roberts, Space Research Centre, Cranfield University, Preprint submitted to Progress in Aerospace Sciences September 7, 2016

- [2] Satellite Drag: Aerodynamic Forces in LEO; Marcin Pilinski; SWx-TREC LASP / University of Colorado 2018-04-25 9th CCMC Community Workshop College Park, Maryland
- [3] Essential spaceflight dynamics and Magnetospherics; Boris V. Rauschenback, Michael Yu. Ovchinnikov, Susan Mckenna-Lawlor; Kluwer Academic Publishers 2003, Print ISBN 978-1-4020-1063-7
- [4] Handbook of Space Technology Edited by Wilfried Ley, Klaus Wittmann and Willi Hallmann © 2009 John Wiley & Sons, Ltd. ISBN: 978-0-470-69739-9
- [5] G.A.Bird, “molecular Gas Dynamics and the Direct Simulation of Gas Flows”, Oxford University Press, 1994
- [6] Bird,G.,URLhttp://sydney.edu.au/engineering/aeromech/dsmc_gab
- [7] Gas–surface interactions and satellite drag coefficients Kenneth Moe, Mildred M. Moe Science and Technology Corporation, 23 Purple Sage, Irvine, CA 92603 Received 6 May 2004; received in revised form 26 July 2004; accepted 18 March 2005
- [8] Abdul Majid “Code for Heating& Hypersonic Aerodynamic Prediction with Re-entry COrridor Estimation” MSc thesis, SUPAERO, Toulouse France 2005
- [9] Marcin D. Pilinski, Brian M. Argrow and Scott E. Palo, “Drag coefficients of satellites with Concave Geometries : Comparing models and observations” Journal of Spacecrafts and rockets, Vol. 48, No. 2, March-April 2011
- [10] E.M. Gaposchkin and AJ. Coster“Analysis of Satellite Drag”, The Lincoln Laboratory Journal. Volume 1. Number 2 (1988).
- [11] Bertin J. John “Hypersonic Aerothermodynamics” AIAA Education Series, second printing, 1994
- [12] Anderson John D Jr. “Hypersonic and High Temperature Gas Dynamics” McGraw-Hill Series in Aeronautical and Aerospace Engineering, 1989
- [13] F. A. Marcos, W. J. Burke, and S. T. Lai. Thermospheric space weather modeling. In Collection of Technical Papers - 38th AIAA Plasmadynamics and Lasers Conference, volume 2, pages 999-1010, 2007.